ELSEVIER

Journal of Nuclear Materials 266–269 (1999) 679–684

journal of nuclear materials

SOL currents and divertor asymmetries on COMPASS-D

C.G. Silva [a,*], S.J. Fielding [b], K.B. Axon [b], M.G. Booth [b]

[a] *Associação Euratom/IST, Centro de Fusão Nuclear, Instituto Superior Técnico 1096 Lisbon Codex, Portugal*
[b] *UKAEA/Euratom Fusion Association, UKAEA Fusion, Culham Science Centre, Abingdon, Oxon OX14 3DB, UK*

Abstract

On COMPASS-D, distortions in the density profile at the divertor target are observed in all discharge phases. These distortions are strongly affected by the toroidal field direction, and for $B_T > 0$ appear as a large asymmetry between the inner and outer divertor regions. In this paper we investigate the effect of both drifts and scrape-off layer (SOL) currents on divertor plasma parameters. Large currents are observed in the divertor region, which change the plasma potential creating large electric fields in the divertor target. The resulting $\mathbf{E} \times \mathbf{B}$ drift is suggested as a possible mechanism causing the observed distortions. A combination of thermoelectrical and Pfirsch-Schlüter terms are proposed as driving mechanisms for the SOL currents.

Keywords: *B*-field reversal; COMPASS-D; Divertor asymmetry; Divertor plasma; Drifts; $\mathbf{E} \times \mathbf{B}$ drift; Electrical currents; SOL currents

1. Introduction

Previous experiments carried out in COMPASS-D [1] and other tokamaks, e.g. JET [2] and Alcator C-Mod [3], have shown large asymmetries and distortions in the divertor target profiles. These distortions directly affect the peak heat load at the target and, for example, are important considerations in the ITER divertor design.

In most single-null divertor tokamaks, divertor profiles show strong variations with the discharge parameters and in particular with the direction of the toroidal magnetic field, B_T. In order to investigate the effects caused by the toroidal field direction, a series of L-mode discharges with both B_T directions and similar core plasma parameters was performed on COMPASS-D.

We report here edge measurements on COMPASS-D (Fig. 1) during L-mode discharges in lower single-null divertor plasmas, using a fast reciprocating Langmuir probe poloidally remote from the *X*-point, and a high spatial resolution (5 mm) array of embedded probes in the divertor target [4] which provide detailed information of the effect on plasma parameters at the boundary. These probes have been operated under a wide variety of discharge conditions, and the collected data, plasma density, electron temperature, SOL current (current at zero voltage) and floating potential, stored in a database.

Radial and poloidal electric fields exist naturally in the scrape-off layer (SOL) and the resulting $\mathbf{E} \times \mathbf{B}$ drift has been suggested as one possible cause of the asymmetry [5] since drifts can change the density distribution at the target, consequently affecting the temperature and heat flux distributions. Recent measurements on COMPASS-D [1,6] have shown the existence of large currents on the divertor target (SOL currents) which significantly influence the radial electric field profile. SOL currents have been observed and investigated in several tokamaks, e.g. JET [7], Alcator C-Mod [3] and JT-60U [8], however, driving mechanisms are not yet fully understood.

2. The effect of field reversal on the divertor parameters

The effect of the field direction on parameters at the divertor has been investigated on COMPASS-D by reversing the toroidal magnetic field and plasma current direction simultaneously, so that the sign of the helicity

* Corresponding author. Tel.: +351 1 841 7696; fax: +351 1 841 7819; e-mail: csilva@cfn.ist.utl.pt.

0022-3115/99/$ – see front matter
PII: S0022-3115(98)00600-X

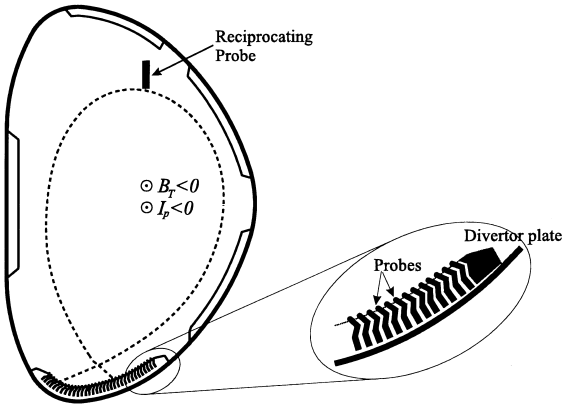

Fig. 1. Poloidal cross-section of COMPASS-D with position of the divertor probe array and reciprocating probe.

of the field lines is unchanged (avoiding exposing different surfaces to plasma bombardment, with possible recycling changes confusing the data). This study has been confined to L-mode discharges, since H-mode is only observed on COMPASS-D for one direction of the field. The toroidal magnetic field direction favourable to H-mode, corresponding to ∇B ion drift down towards the X-point, is defined as negative (see Fig. 1).

In L-mode discharges the B_T direction has a substantial effect on the target density, as shown in Fig. 2. The density profile is approximately symmetric for $B_T < 0$, while for $B_T > 0$ a large density imbalance is observed. This results in a strong outboard/inboard pressure imbalance since the temperature profile is approximately symmetric. Furthermore, for $B_T < 0$ distortions in the density profile are observed, mainly in the outer divertor region. These are also seen in H-mode discharges, where they are more clearly defined. In contrast, the reversal of the B_T direction has a smaller effect on the temperature profile. For $B_T < 0$ the divertor plasma is hotter in the outboard region, and reversing B_T leads to a more even temperature distribution. Because there are opposing changes in the n_e and T_e distributions when the magnetic field is reversed, the heat flux distribution is similar for both directions, with higher power flowing to the outer target.

As a general trend, in single-null divertor plasmas on other devices [2,3] the outer divertor target receives a higher power flux than the inner one, in agreement with COMPASS-D results. In most machines, however, more symmetric power flux profiles are observed for $B_T > 0$, contrary to COMPASS-D where the opposite is observed. This originates from the large density asymmetry observed on COMPASS-D for $B_T > 0$, which is not observed in other devices.

Higher electron temperature at the outer divertor region is expected from geometrical considerations – the outboard SOL has a larger surface area, by virtue of its

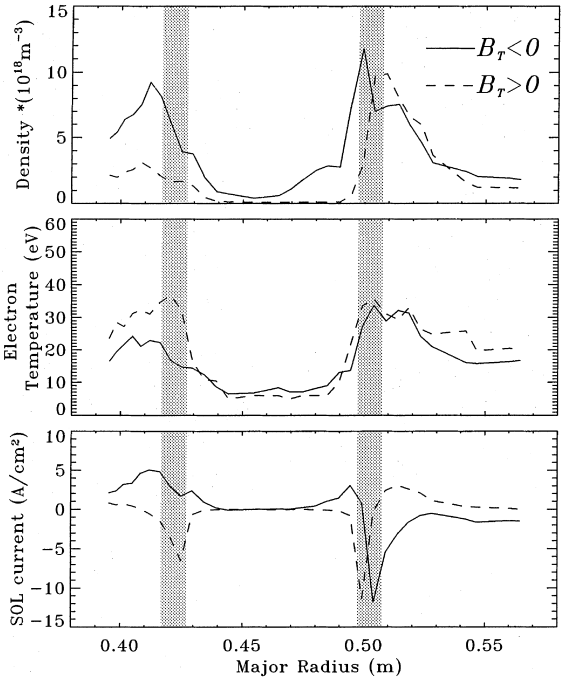

Fig. 2. Profiles of n_e, T_e and SOL currents for $B_T < 0$ (#21483) and $B_T > 0$ (#21494). The strike-point positions given by DFIT (equilibrium reconstruction code) are indicated by the grey bars. The ion drift side is located at the outboard region for $B_T > 0$.

greater major radius. This shifts the stagnation point towards the outer side creating a temperature asymmetry between the two sides in favour of the outer one [9]. For $B_T > 0$ this asymmetry is not observed because of the large density imbalance. The larger density at the outer divertor region means higher recycling, and therefore a temperature reduction, in this region. The higher recycling is corroborated by camera data which shows that the visible radiation in the outboard side is dominant for $B_T > 0$.

Divertor target probes operated with zero applied voltage show high current densities (Fig. 2), which integrate across the divertor target to approximately zero. These currents too are substantially affected by the magnetic field direction. In the common flux region (the region outside of the separatrix), divertor currents appear to flow from the electron to the ion drift side. However, in the private flux region narrow current layers with the same direction at both strike-points are observed, which always change sign with change in B_T direction. The sheath transmission, and consequently the heat flux density at the target, change as a consequence of these non-ambipolar flows to the surface. The sheath transmission factor, γ, is nearly a minimum at the floating potential, $\gamma_0 \simeq 7$, thus a current flow, j, across the sheath can only increase γ. However, the total power

flow to the target is only marginally increased (< 5%) over the ambipolar value.

3. Drifts effects at the divertor

The direction of the toroidal field determines the direction of cross-field particle drifts. Therefore, imbalances that are sensitive to the field direction are almost certainly a reflection of the drifts [5]. The $\mathbf{E} \times \mathbf{B}$ drift is suggested as one possible mechanism causing the observed distortions in divertor profiles.

As shown in Fig. 2, on COMPASS-D both density and SOL current distribution are strongly influenced by the B_T direction. In this section, distortions of the density profile at the divertor target are investigated for both field directions and an explanation is presented, based on the SOL currents and the $\mathbf{E} \times \mathbf{B}$ drift.

Our co-ordinate system is the same used in [3]. Directions are conveniently labelled as 'radial', 'parallel' and 'poloidal' referring to the vectorial directions: $\nabla\psi$, $\mathbf{B}$ and $\mathbf{B} \times \nabla\psi$, where ψ is the poloidal flux. The 'poloidal' direction, under this nomenclature, possesses a small, but ignorable toroidal component. The parallel direction also has an important component in the poloidal plane.

In plotting divertor profiles the probes position are projected along the major radius. A equilibrium reconstruction code should be used to calculate radial profiles at the divertor target from probe measurements. However, this mapping does not change target profiles significantly. Since only a qualitative analysis is presented in this paper, a simple projection of the divertor profiles onto the major radius is used.

3.1. B_T negative

For $B_T < 0$ a distortion in the density profile is usually observed in the outer divertor region (see Fig. 3). Such structure, which is only identified because of the high spatial resolution of the divertor probes is also seen in camera images of the divertor region, and hence is not thought to be a measurement artefact of the probes.

As shown before, high current densities with large spatial variations are observed in the divertor target, particularly near the strike-points (see Fig. 2). Such currents can only be sustained if the sheath potential relaxes from its ambipolar value. Allowing for a current density, $j_\parallel$, in the target, the sheath potential, Φ_s, is given by

$$\Phi_s - \Phi_t = \Phi_s^a - \frac{T_e}{e} \ln\left(1 - \frac{j_\parallel}{j_{sat}^+}\right), \quad (1)$$

where Φ_t and Φ_s^a are respectively the target potential and the sheath potential assuming ambipolarity. Neglecting the secondary electron emission (Φ_s^a is independent of the s.e.e for shallow field lines [10]) and assuming $T_e \approx T_i$, $\Phi_s^a \approx 3T_e/e$. The SOL current is detected when

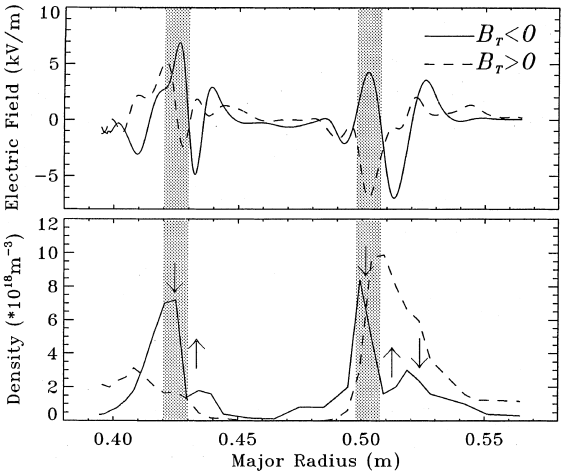

Fig. 3. Typical E_r and n_e profiles for $B_T < 0$ (#17769) and $B_T > 0$ (#21494). The directions of the $\mathbf{E}_r \times \mathbf{B}$ drift flow for $B_T < 0$ are also shown (arrows).

the probe is at zero (i.e. at target potential). Thus, as a result of the large spatial variation in the SOL current, the sheath potential also varies across the divertor target and a large electric field is observed, (see Fig. 3). Using the T_e and V_f profiles measured by the divertor probes it is possible to obtain the plasma potential and thus the radial electric field. The radial electric field cause a poloidal $\mathbf{E}_r \times \mathbf{B}$ drift which changes the flow parallel to the magnetic field creating distortions in the divertor profiles. When the electric field is negative, the poloidal $\mathbf{E}_r \times \mathbf{B}$ drift is directed away from the target, resulting in a plasma outflux. In the outer target there is a plasma outflux (decreasing n_e) in both sides of the strike-point, causing the observed distortion. The correlation between the $\mathbf{E}_r \times \mathbf{B}$ drift direction and the observed distortions is clear.

The magnitude of the poloidal $\mathbf{E}_r \times \mathbf{B}$ particle flux can be estimated as: $\Gamma^d = nE_r/B$. Parallel flow at the ion sound speed causes a poloidal flux: $\Gamma^\parallel = nc_sB_\theta/B$ ($\propto j_{sat}^+$). The ratio of the two fluxes is: E_r/c_sB_θ. This ratio can be of the order of unity, therefore strongly affecting the overall flux pattern in the divertor region.

3.2. B_T positive

As shown in Fig. 2, for $B_T > 0$ the distortions in the density profile appear as a large asymmetry between the inner and outer divertor regions (up to a factor of 4), which have been investigated in detail previously on COMPASS-D [1]. The radial electric field resulting from the SOL current (Fig. 3), can again explain the observed distortions. In the common flux region, the electric field is positive in the inboard side and negative in the outboard side, close to the separatrix. Thus, the resulting poloidal $\mathbf{E}_r \times \mathbf{B}$ drift is directed from the inner to the

outer divertor region, causing the large asymmetry observed. Note that for $B_T > 0$ a positive electric field means now a plasma outflux from the target. In addition to the radial electric field, there is a poloidal electric field (E_θ) along the SOL [1] whose average value is derived by comparing upstream and target potentials. Radial fluxes, caused by the poloidal electric field ($\mathbf{E}_\theta \times \mathbf{B}$), will again increase the density in the outer divertor region for $B_T > 0$.

The $\mathbf{E} \times \mathbf{B}$ drifts are in the right direction to explain the large asymmetry observed for $B_T > 0$, since both its radial and poloidal components are directed towards the outer divertor region.

4. SOL currents

Parallel currents in the divertor scrape-off layer (SOL currents) were first predicted by Harbour [9] and have been observed and investigated in several tokamaks, e.g. JET [7], Alcator C-Mod [3] and JT-60U [8].

It was shown in the previous section that divertor target profiles are strongly influenced by the $\mathbf{E} \times \mathbf{B}$ drifts, where the electric field is largely determined by the SOL current profile. Thus, a full identification of the physical mechanisms driving these currents can contribute significantly to understanding, and probably controlling, the divertor profiles.

On COMPASS-D, divertor target probes operated with zero applied voltage show, as a rule, high current densities (up to 15 A/cm^2). Close to the strike-points, narrow current layer features with large current density are observed. These too are substantially affected by the magnetic field direction. Some of the current layers are possibly even narrower than those observed since the radial dimension of the probes (2 mm) is comparable to the width of the narrowest profiles at the target.

Several mechanisms driving parallel currents in the SOL have been examined by Chankin [11], including the thermoelectric effect and pressure related Pfirsch–Schlüter currents. Due to the variety of physical mechanisms that may cause current flow, the resultant structure of target profiles of electric currents can be rather complex and difficult to resolve in the experiment.

Possible driving terms for the current are temperature and pressure gradients along the magnetic field (thermoelectric effect) [12]. Fig. 4(a) shows the SOL current for $B_T < 0$ and an overlay of the calculated thermoelectric current. The predicted thermoelectric current was calculated, on each flux tube, from the SOL conductivity, $\bar{\sigma}_\parallel$, and the parallel temperature and pressure gradients, derived from the electron temperature and pressure measured by the divertor probe array at both ends of the flux tube and computed connection lengths. Data from the outer divertor region was mapped onto the inner region using the reconstructed magnetic field

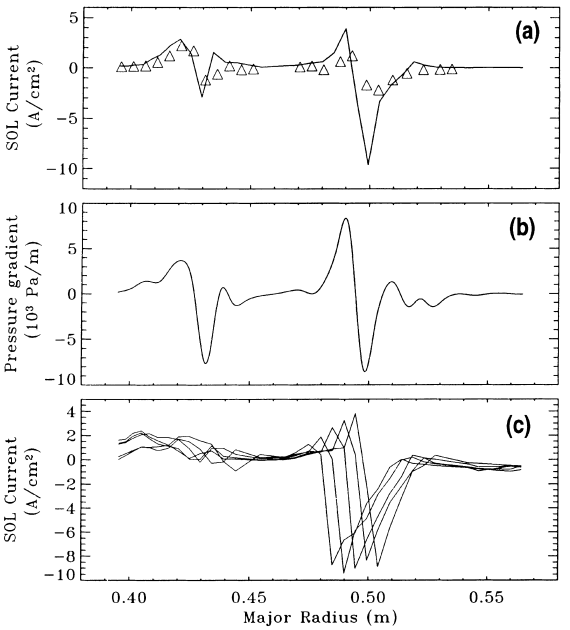

Fig. 4. Profile of SOL current for $B_T < 0$ (#21480) measured by the divertor probe array (a). The thermoelectric current computed from temperature and pressure gradients is also shown (triangles). Derived radial pressure gradient at the divertor target (b), again for $B_T < 0$. Variation of the SOL current with distance between strike-points (c).

structure given by DFIT (a filament-based code). Spitzer conductivity was assumed for $\bar{\sigma}_\parallel$ taking for the average SOL parameters the values measured by the reciprocating probe (typically $n = 5 \times 10^{18}$ m^{-3} and $T_e = 50$ eV). The calculated and measured currents agree quite well far from the strike-points; however, close to the strike-points the amplitude of the observed current is larger than predicted by the thermoelectric effect and cannot be totally explained by this.

Pressure related currents, namely Pfirsch–Schlüter currents, have recently been suggested as an explanation of similar narrow current density peaks observed in JET [13]. Schaffer et al. [13] showed that these pressure related currents flow in a narrow zone near the strike-points, with opposite directions for the two different field directions. Pfirsch–Schlüter currents are predicted to be proportional to the pressure gradient at the divertor target ($\partial p/\partial \psi$) and to the radial separation of the inner and outer separatrix strike-points. The sign is expected to depend on the B_T direction. The Pfirsch–Schlüter current is most likely to be separable from the thermoelectric current in the private flux region, since the thermoelectric current is small there and the Pfirsch–Schlüter current is expected to be large, owing to the steepness of the profiles in the private region.

Fig. 4(b) shows the radial pressure gradient, $\nabla_r p$, (assuming $p_i = p_e$, since the ion contribution is not

measured) at the divertor target, again for $B_T < 0$. The correlation between $\nabla_r p$ and the SOL current is manifestly clear. The dependence of the current to the private flux region on the distance between strike-points was also investigated moving the plasma up and down during the discharge. For Ohmic L-mode discharges, the total current to the private region was observed to increase roughly linearly with increase in distance between strike-points (see Fig. 4(c)), and its sign to depend on the B_T direction. Thus, a qualitative agreement between the Pfirsch–Schlüter current predictions and the observed currents close to the strike-points was found. It seems probable, therefore, that the measured SOL current on COMPASS-D principally consists of a combination of thermoelectrical and Pfirsch–Schlüter terms, both parallel to the magnetic field.

The narrow current layers observed in the private region can easily be explained by the ∇B drift [11]. For B_T positive, the ion ∇B direction is away from the target and a negative charge is flowing into the private region. Due to short connection lengths in the private region this should create narrow negatives peaks of current just inside the separatrix. Similarly, positive peaks should be created for B_T negative. This result is not surprising because the Pfirsch–Schlüter current exists due to the short circuiting, along **B**, of the polarization charges resulting from the ∇B drift.

In the private region, the magnitude of the positive current peaks observed for $B_T < 0$ are much smaller than the negative ones observed for $B_T > 0$, as shown in Fig. 2. The magnitude of the SOL current is limited by the plate saturation current, i.e. the current density can not be greater than the ion saturation current density, j_{sat}^+, at the ion-collecting plate [Eq. (1)], or smaller than the electron saturation current density, j_{sat}^-, at the electron-collecting plate, $j_{sat}^- < j < j_{sat}^+$. Thus, positive currents are limited by j_{sat}^+, which is very small in the private flux region, while for negative currents the limitation is much weaker, since on COMPASS-D $j_{sat}^- \simeq 10 j_{sat}^+$ [4]. However, the total current to the private flux region is roughly the same for both field directions because positive peaks are much wider than negative ones.

It has been qualitatively shown in this paper that SOL currents strongly influence divertor target density profiles, consequently affecting the pressure distribution. However, SOL currents are also affected by the pressure profile since both driving mechanisms, thermoelectric effect and Pfirsch–Schlüter currents, depend on the pressure profile. The complexity of this problem means that 2D numerical codes have to be used in order to describe the experimental results. Electric currents in the scrape-off layer and drifts should be incorporated into these numerical codes in order to quantitatively assess their effect in the divertor target profiles. Efforts are already in progress (see e.g. [14]).

Since divertor target profiles are largely determined by the electric field at the target, divertor biasing could be used in order to tailor this field profile, and thus, control divertor profiles. Unfortunately, this could not be tested on COMPASS-D due to the configuration of the divertor target tiles.

5. Summary

On COMPASS-D, distortions in the density profile at the divertor target are observed which are strongly affected by the toroidal field direction. The $\mathbf{E} \times \mathbf{B}$ drift offers a possible explanation for these distortions for both field directions since it can change the density distribution at the target. The large currents observed in the divertor region, which change the plasma potential creating large electric fields in the divertor target, significantly influence the divertor profiles. It seems probable, that the measured SOL current on COMPASS-D principally consists of a combination of thermoelectrical and Pfirsch–Schlüter terms, both parallel to the magnetic field.

Acknowledgements

This work is jointly funded by the UK Department of Trade and Industry and Euratom. C.G. Silva was supported by a EURATOM fellowship.

References

[1] C.G. Silva, S.J. Fielding, K.B. Axon, M.G. Booth, Plasma Phys. Control. Fusion 40 (1998) 1159.
[2] A.V. Chankin, D.J. Campbell, S. Clement, S.J. Davies, L.D. Horton, J. Lingertat, A. Loarte, G.F. Matthews, R.D. Monk, R. Reichle, G. Saibene, M. Stamp, P.C. Stangeby, Plasma Phys. Control. Fusion 38 (1996) 1579.
[3] I.H. Hutchinson, B. LaBombard, J.A. Goetz, B. Lipschultz, G.M. McCracken, J.A. Snipes, J.L. Terry, Plasma Phys. Control. Fusion 37 (1995) 1389.
[4] C.G. Silva, S.J. Fielding, K.B. Axon, M.G. Booth, Contrib. Plasma Phys. 38S (1998) 47.
[5] P.C. Stangeby, A.V. Chankin, Nucl. Fusion 36 (1996) 839.
[6] S.J. Fielding, K.B. Axon, M.G. Booth, R.J. Buttery, J. Dowling, D. Gates, C. Hunt, C. Silva, M. Valovic, J. Nucl. Mat. 241–243 (1997) 902.
[7] P.J. Harbour et al., J. Nucl. Mater. 162–164 (1989) 236.
[8] A. Kumagai, N. Asakura, K. Itami, M. Shimada, M. Nagami, Plasma Phys. Control. Fusion 39 (1997) 1189.
[9] P.J. Harbour, Contrib. Plasma Phys. 28 (1988) 417.
[10] R. Chodura, Physics of Plasma–Wall Interactions in Controlled Fusion, Plenum, New York, 1986, p. 99 .
[11] A.V. Chankin, J. Nucl. Mater. 241–243 (1997) 121.
[12] G.M. Staebler, F.L. Hinton, Nucl. Fusion 29 (1989) 1820.

[13] M.J. Schaffer, A.V. Chankin, H.Y. Guo, G.F. Matthews, R. Monk, Nucl. Fusion 37 (1997) 83.
[14] G.J. Radford, A.V. Chankin, G. Corrigan, R. Simonini, J. Spence, A. Taroni, Proceedings of 24th EPS Conference on Controlled Fusion and Plasma Physics, Part I, Berchtesgaden, 1997, vol 21A, p. 125.